A Comparative Study of LES Models Under Location Uncertainty

P. CHANDRAMOULI[a], D. HEITZ[a,b], E. MÉMIN[a], S. LAIZET[c]

a. INRIA, Fluminance group, Campus universitaire de Beaulieu, F-35042 Rennes Cedex, France
pranav.chandramouli@inria.fr
b. Irstea, UR OPAALE, F-35044 Rennes Cedex, France
c. Department of Aeronautics, Imperial College London, London, United Kingdom

Résumé :

Les modèles sous incertitude de localisation récemment introduits par Mémin [16] fournissent une nouvelle perspective concernant le développement de modèles aux grandes échelles (LES) pour l'étude d'écoulements turbulents. Ces modèles sont bâtis à partir d'équations de conservation stochastiques dérivées d'une expression aléatoire du théorème de transport de Reynolds. A l'instar des modèles classiques, ces modèles incluent un terme de dissipation sous-maille. Un terme de correction additionnel, du à l'advection des grandes échelles par les petites échelles. Ce biais de vitesse artificiellement introduit dans les modèles stochastiques par MacInnes et Bracco [14], est ici rigoureusement justifié. Ces deux termes découlent d'une hypothèse de décorrélation en temps des petites échelles à l'échelle résolue et sont définis à partir du tenseur d'auto-correlation des petites échelles qui doit être modélisé. Plusieurs expressions de ce tenseur construites à partir de variances empiriques locales ou à partir d'une equivalence avec le tenseur sous-maille de Smagorinsky ont ainsi été étudiées. Les performances de ces modèles ont été évalués dans le cas de deux écoulements très bien documentés dans la littérature : l'écoulement de sillage en aval d'un cylindre à Re 3900 et un écoulement de canal lisse à Re_τ 395. Ces deux écoulements rassemblent des caractéristiques essentiels des écoulements turbulents et restent associés à une complexité numérique raisonnable. Ils constituent donc des banc-tests parfaits. Une comparaison avec divers modèles sous-maille classiques indique une performance supérieure des modèles sous incertitude de position.

Abstract :

The models under location uncertainty recently introduced by Mémin [16] provide a new outlook on LES modelling for turbulence studies. These models are derived from the stochastic conservation equations using stochastic calculus. These stochastic conservation equations are similar to the filtered Navier-Stokes equation wherein we observe a sub-grid scale dissipation term. However, in the stochastic version, an extra term appears, termed as "velocity bias", which can be treated as a biasing/modification of the large scale advection by the small scales. This velocity bias, introduced first in stochastic models by MacInnes and Bracco [14] albeit artificially, appears here automatically through a decorrelation assumption of the small scales at the resolved scale. All sub-grid contributions for the stochastic models are defined by the small scale velocity auto-correlation ($a = \sigma\sigma^T$) which can be modelled through a Smagorinsky equivalency or by a local variance calculation. In this study, we have worked towards

verifying the applicability and accuracy of these models in two well-studied cases namely that of flow over a circular cylinder at Re $\sim$ 3900 and smooth channel flow at $Re_\tau \sim 395$. Both these flows have been extensively studied in literature and provide well-established data sets for model comparison. In addition, these flows display numerous important characteristics of turbulence flows that needs to be captured efficiently by the model. This combined with the flow associated numerical complexities makes these the ideal flow for model study. A comparison of the models indicates a statistical improvement in the models under location uncertainty compared with classical deterministic models for both flows.

Mots clefs : Large eddy simulation, Stochastic models, Wake flow around a circular cylinder, Channel flow

1 Introduction

Large Eddy Simulations (LES) are an effective cost reduction technique for performing simulations of flows that are computationally too expensive for a Direct Numerical Simulation (DNS). In an LES framework, a low pass filter is applied splitting the flow field into the large scale flow which is resolved by the simulation and the sub-grid scale (SGS) flow which is modelled using appropriate models. The filtered mass conservation and Navier-Stokes equations for incompressible flow are given as :

$$\nabla \cdot \boldsymbol{u} = 0, \tag{1}$$

$$\frac{\partial \bar{\boldsymbol{u}}}{\partial t} + \bar{\boldsymbol{u}} \cdot \nabla \bar{\boldsymbol{u}} = -\frac{1}{\rho}\nabla \bar{p} + \nu \nabla^2 \bar{\boldsymbol{u}} - \nabla \cdot \boldsymbol{\tau}, \tag{2}$$

where ($\bar{}$) indicates a filtered field, $\boldsymbol{u}$ stands for the flow field, ρ is density of the fluid, p refers to flow pressure field, ν is kinematic viscosity of the fluid and $\boldsymbol{\tau}$ stands for sub-grid scale stress tensor that needs to be modelled. The first SGS model for representing $\boldsymbol{\tau}$ was given by Joseph Smagorinsky in his pioneering work on atmospheric air currents [28]. Following his work, considerable research in LES and SGS modelling has resulted in a myriad of models for representing the SGS flow field and its contributions. With ever increasing computational resources and accurate SGS models, LES is fast becoming a norm for simulations in the present day scenario.

The application of a filter on the flow field effectively reduces the cost of the simulation, however, this is associated with a loss in accuracy. For an accurate simulation, the SGS models need to capture the physics of the small scale flow field and its interaction with the resolved field accurately. One of the simplest models for LES was proposed by Smagorinsky (Smag) based on the equivalency of energy production and dissipation at the small scales. Combining Boussinesq's eddy viscosity hypothesis with Prandtl's mixing length hypothesis, Smagorinsky developed a model to characterise the SGS flow contribution ($\boldsymbol{\tau}$).

$$\tau_{ij} = -2\nu_t \bar{S}_{ij}, \tag{3}$$

$$\nu_t = (C_s \Delta)^2 \bar{S}, \tag{4}$$

where $\bar{S}$ is the filtered strain rate, ν_t is the local eddy viscosity, C_s is an arbitrary constant, and Δ is the filter width.

The drawbacks of the Smagorinsky model namely the user-specified constant, the prevention of energy

backscatter, and the non-zero value for ν_t for laminar flow were addressed by researchers through modifications to the classical version of the Smagorinsky model and through other approaches. The Dynamic Smagorinsky model by Germano [5], addressing the ad-hoc constant issue by using a bigger test filter and calculating the Smagorinksy coefficient, is another well established version of the Smagorinksy model. The Wall Adaptive Local-Eddy visocsity (WALE) model developed by Nicoud and Ducros [19] is another established SGS model which argues the importance of the rotational strain rate in ν_t calculations. They proposed an eddy viscosity equation incorporating irrotational and rotational strain rate while maintaining a similar form to the classic Smagorinsky model.

$$\nu_t = (C_w \Delta)^2 \frac{(\varsigma^d_{ij}\varsigma^d_{ij})^{3/2}}{(\bar{S_{ij}}\bar{S_{ij}})^{5/2} + (\varsigma^d_{ij}\varsigma^d_{ij})^{5/4}}, \tag{5}$$

$$\varsigma^d_{ij}\varsigma^d_{ij} = \frac{1}{6}(S^2S^2 + \Omega^2\Omega^2) + \frac{2}{3}S^2\Omega^2 + 2IV_{S\Omega}, \tag{6}$$

where $S^2 = \bar{S_{ij}}\bar{S_{ij}}, \Omega^2 = \bar{\Omega_{ij}}\bar{\Omega_{ij}}, IV_{S\Omega} = \bar{S_{ik}}\bar{S_{kj}}\bar{\Omega_{jl}}\bar{\Omega_{li}}$, Ω stands for the rotational strain rate and C_w is the WALE constant. This constant, unlike C_s, is an universal constant and holds for all cases.

The above described set of models are all based on the Boussinesq approximation. Other approaches to SGS modelling includes the so called kinetic-energy models which calculate the SGS viscosity based on the SGS kinetic energy, determined by solving an additional scalar transport equation. The approaches of Deardorff [2] and Schumann [26] fall under this category. Other broad categories of SGS modelling include the wavenumber dependant eddy viscosity calculations in spectral space, explicit reconstruction of the SGS velocity field, or one-dimensional turbulence models. Another fundamentally different approach to SGS modelling is implicit LES where in the SGS dissipation is numerically introduced instead of using physical models [11].

While all the above models ensue from a deterministic modelling, another well-explored approach to SGS modelling is stochastic modelling. In this approach, the large scale flow field is considered to incorporate small scale random uncertainties. The literature on defining the random uncertainties for these models can be broadly split into two approaches. The first involves the representation of the large scale velocity in the Fourier domain which is closed using a Langevin equation [9, 12]. The second approach introduces a random forcing directly in the Navier-Stokes equation [1, 15, 27]. In the same vein as direct forcing, an alternate approach to stochastic modelling based on stochastic conservation equations introduced by Memin [16] is considered in this study - the derivation of such a model in a geophysical context as well as its application can be found in [22, 23, 24]. A similar approach was also done by the recent works of Holm [8]. The next section describes the methodology adopted by Memin and the model formulation in an LES context. This is followed by a section on model results for two turbulent flows. Finally, a section of concluding remarks follows.

2 Models under Location Uncertainty

Memin's stochastic models (henceforth referred to as Models under Location Uncertainty) are built on a stochastic approach to the conservation equations. Instead of introducing random noise in a deterministic formalism, Memin derived the conservation equations in a stochastic framework with a flow velocity split into a large scale smooth component ($\boldsymbol{w}$) and a small scale noise defined by a Brownian function ($\boldsymbol{\sigma}\dot{\boldsymbol{B}}$). A stochastic version of the Reynolds Transport Theorem is used to derive the stochastic mass and momentum conservation equations given in (7) and (9) (For full derivation please refer to [16, 22]).

Assuming incompressibility reduces the stochastic mass conservation equation (7) to a set of constraints as given in (8).

$$d_t\rho_t + \boldsymbol{\nabla}\cdot(\rho\tilde{\boldsymbol{w}})dt + \boldsymbol{\nabla}\rho\cdot\boldsymbol{\sigma}\, d\boldsymbol{B}_t = \frac{1}{2}\,\boldsymbol{\nabla}\cdot\,(\boldsymbol{a}\boldsymbol{\nabla}q)dt, \tag{7}$$

$$\boldsymbol{\nabla}\cdot\,(\boldsymbol{\sigma}d\boldsymbol{B}_t) = 0, \quad \boldsymbol{\nabla}\cdot\,\widetilde{\boldsymbol{w}} = 0, \tag{8}$$

$$\left(\partial_t\boldsymbol{w} + \boldsymbol{w}\boldsymbol{\nabla}^T(\boldsymbol{w} - \frac{1}{2}\boldsymbol{\nabla}\cdot\boldsymbol{a}) - \frac{1}{2}\sum_{ij}\partial_{x_i}(a_{ij}\partial_{x_j}\boldsymbol{w})\right)\rho = \rho\boldsymbol{g} - \boldsymbol{\nabla}p + \mu\Delta\boldsymbol{w}, \tag{9}$$

where $\tilde{\boldsymbol{w}} = \boldsymbol{w} - \frac{1}{2}\boldsymbol{\nabla}\cdot\boldsymbol{a}$ stands for the modified advection which results from the inter-dependancy between the two scales of flow velocity, σ is the square root of the random field covariance, and $\boldsymbol{a}$ is the diffusion tensor obtained from the small-scale velocity auto-correlations multiplied by the decorrelation time - this give units of m^2/s, same as that of a dissipation tensor. Note that this stochastic approach to modelling does not rely on any a priori hypothesis such as the Boussinesq's eddy viscosity assumption. The only assumption in the derivation is brought by the decorrelation assumption of the small scale noise at the resolved time-scale. The mass conservation constraints for an incompressible flow enforce a divergence criterion on the small scale noise field as well as on the large scale velocity field via the velocity bias $\tilde{\boldsymbol{w}}$.

The momentum conservation equation is analogous to the filtered Navier-Stokes equation, i.e. it has an extra dissipation term marking the contribution of the small scales while the dynamics of the large scales are resolved. However, a major deviation between the two formulations is the presence of the velocity bias which modifies advection by taking into account the effect of the small scale. Such modification of the advection has been for long considered in Langevin models of inertial particles. The form of this velocity bias is however empirically introduced in [14]. Nevertheless, it is strictly to note that such a bias is to the authors knowledge never been included in LES model with the exception of the so-called "bollus" velocity in the Gent Mcwilliams sub-grid tensor for meso-scale oceanic models [4]. The small scale contributions to the equation are accounted for by the diffusion tensor $\boldsymbol{a}$ which needs to be modelled via suitable methodologies.

One such method is based on the classic Smagorinsky (Smag) model where in the correlation tensor is defined similar to the eddy viscosity in the Smagorinsky model. This proposed Stochastic Smagorinsky model (StSm) is modelled as :

$$\boldsymbol{a}(\boldsymbol{x},t) = C||\boldsymbol{S}||\mathbb{I}_3, \tag{10}$$

where C is a constant (set same as the Smagorinsky constant), $||\boldsymbol{S}||$ is the strain rate norm, and $\mathbb{I}_3$ stands for 3×3 identity matrix. Such a model while identical to Smagorinsky formulation, differs in the implementation via the slightly modified dissipation term as well as the extra velocity bias term.

Another methodology for specifying $\boldsymbol{a}$ can be through statistical techniques where in $\boldsymbol{a}$ can be represented by a local covariance calculated on the large scale resolved component. Two methods can be envisaged for a local covariance computation, namely spatial covariance (StSp) and temporal covariance (StTe). The formulation for the two methods are given below :

StSp :

$$\boldsymbol{a}(\boldsymbol{x},t) = \frac{1}{|\Gamma|-1} \sum_{x_i \in \Gamma(x)} (\boldsymbol{w}(x_i,t) - \bar{w}(x,t))(\boldsymbol{w}(x_i,t) - \bar{w}(x,t))^T C_{st}, \tag{11}$$

StTe :

$$\boldsymbol{a}(\boldsymbol{x},t) = \frac{1}{|\alpha|-1} \sum_{t_i \in \alpha(t)} (\boldsymbol{w}(x,t_i) - \bar{w}(x,t))(\boldsymbol{w}(x,t_i) - \bar{w}(x,t))^T C_{st}, \tag{12}$$

where, $\bar{w}$ stands for the empirical mean around the arbitrarily selected local neighbourhood defined by Γ for StSp and α for StTe. The constant C_{st} is defined as [7] :

$$C_{st} = \left(\frac{L}{\eta}\right)^{\frac{5}{3}} \tau_L, \tag{13}$$

where L is the simulation mesh size, η is the Kolmogorov length scale and τ_L is the decorrelation time for the small scale noise which for the purpose of this study has been set as the simulation time step. It can be verified that the resulting diffusion tensor a has the dimension of an eddy viscosity (m^2/s).

It is interesting to note that while the proposed stochastic formulation does not involve a filtering approach like in LES, the split of the flow field into a large scale and small scale component, and the modelling of dissipation and other contributions of the small scale field are similar to LES modelling.

The next section analyses the performance of the models under location uncertainty for two turbulent flows, namely channel flow at $\mathrm{Re}_\tau \sim 395$ and flow around a cylinder at $\mathrm{Re} \sim 3900$.

3 Results

3.1 Channel Flow at $\mathrm{Re}_\tau \sim 395$

Channel flow has been useful as a research tool for numerous decades ever since a complete data set was provided by [18]. The simplicity of the flow and ease of simulation combined with the turbulent characteristics of the flow close to the wall of the channel makes it an ideal flow for performing model studies. The performance of the models under location uncertainty has been analysed using channel flow at a friction velocity based Reynolds number (Re_τ) of 395. In addition, the model results have been compared with the Smag model as well as the WALE model. The interesting aspect of this study is not just in the range or type of models studied but also on the simulation parameters of the flow (see table 1). The LES has been performed on a grid considerably coarser than the reference grid. A coarse grid for an LES leads to a computationally less expensive simulation which opens avenue of interesting research. One such interesting avenue is Data Assimilation (DA) where recent research has shown good results for DNS in 2D and for 3D at low Reynolds number [25, 6]. An accurate coarse LES could lead to 3D DA studies at higher Reynolds numbers and for more realistic flows.

All simulations were performed using a parallelised flow solver, Incompact3d, developed by [10]. Incompact3d simulates the incompressible Navier-Stokes equations using sixth order finite difference methods (the schemes are described in [13]). For more details about the flow solver please refer to [10]. The LES models, namely Smag, WALE, StSm, StSp, StTe, were incorporated in to Incompact3d which has no inherent model. The constant for Smag and StSm for this flow was set at 0.065 [17] while the constant for WALE was set as 0.5 [19]. A $7 \times 7 \times 7$ local spatial neighbourhood was considered for StSp while a temporal neighbourhood of 7 was considered for StTe. The constant for StSp and StTe are defined based

	$n_x \times n_y \times n_z$	$l_x \times l_y \times l_z$	Δx	Δy	Δz	Δt
LES	48×81×48	6.28×2×3.14	0.13	0.005-0.12	0.065	0.002
Ref	256×257×256	6.28×2×3.14	0.024	0.0077	0.012	-

TABLE 1 – Channel flow parameters.

Model	Reference	Smag	Wale	StSm	StSp	StTe
Re_c	10323	12000	10900	11000	10200	10200

TABLE 2 – Centreline Reynolds number for different SGS models.

on the DNS mesh size, the LES resolution and the LES time step (see eq. (13)). The mesh is stretched in the wall normal (y) direction in order to provide more points in the vicinity of the wall.

Incompact3d uses as input the center-line based Re (Re_c) while the reference data is available for a friction velocity based Re. This poses a numerical problem as the friction velocity for a given Re_c cannot be predicted before simulation and hence an iterative methodology has to be employed. A initial guess for Re_c, based on theoretical calculations, is used to simulate the flow following which the friction velocity and Re_τ are calculated. Re_c is then adjusted based on the value of Re_τ obtained and the simulation is re-run until a $Re_\tau \sim 395$ is obtained. The final Re_c values for each models are tabulated in table 2. All simulations are run until convergence and symmetry is established along the wall normal direction. The statistics are collected over 50000 time steps and averaged along the streamwise (x) and spanwise (z) directions and normalised with respect to friction velocity and Re_τ. All statistics are shown for half channel height to avoid redundancy due to symmetry. The results are analysed below.

Figure 1 shows the mean velocity profile (the log law of the wall) for the channel. The iterative methodology for determining Re_c has biased the statistics for Smag due to its inherent inability to perform well close to the wall - the resultant Re_c is much higher than the theoretical value leading to a more energetic flow. This bias is corrected moderately by StSm however, the performance of StSp and StTe is better than all other models in comparison with the reference DNS.

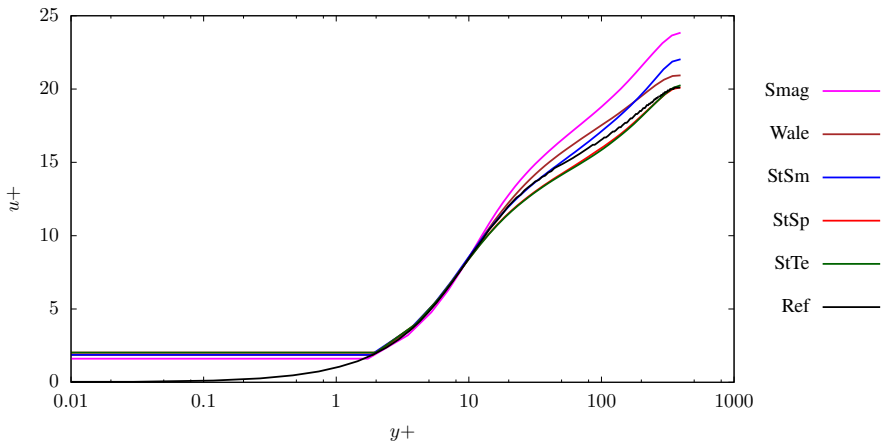

FIGURE 1 – Mean velocity profile for turbulent channel flow at Re_τ = 395

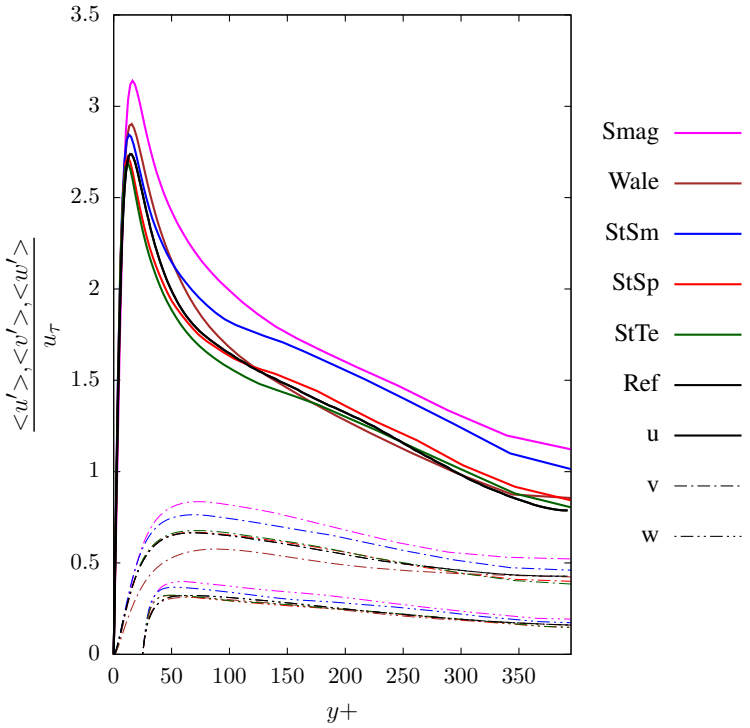

FIGURE 2 – Velocity fluctuation profiles for turbulent channel flow at Re_τ = 395

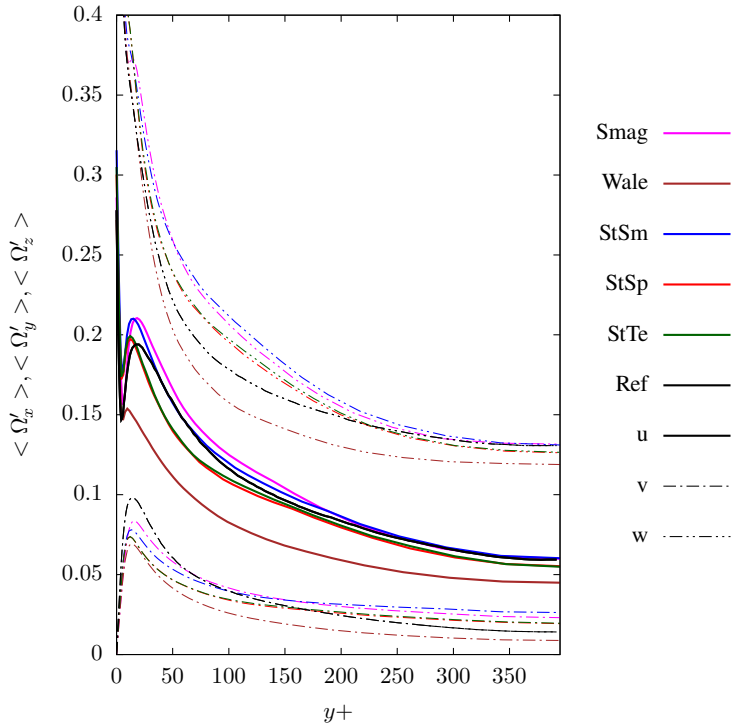

FIGURE 3 – Vorticity (Ω) fluctuation profiles for turbulent channel flow at Re_τ = 395

	Re	$n_x \times n_y \times n_z$	$l_x/D \times l_y/D \times l_z/D$	$\Delta x/D$	$\Delta y/D$	$\Delta z/D$	$U\Delta t/D$
cLES	3900	241×241×48	20×20×3.14	0.083	0.024-0.289	0.065	0.003
PIV - Parn	3900	160×128×1	3.6×2.9×0.083	0.023	0.023	0.083	0.01
LES - Parn	3900	961×961×48	20×20×3.14	0.021	0.021	0.065	0.003

TABLE 3 – Wake flow parameters.

Figure 2 and figure 3 display the velocity and vorticity fluctuation profiles respectively. The statistics have been shifted appropriately in order to maintain visual clarity. A similar trend as for mean velocity profile is observed in the velocity fluctuation profiles. Smag and StSm both over-predict all profiles. Wale, StSp and StTe models predict accurately the velocity fluctuation profiles but an opposite behaviour is seen between Wale model and the other two - an over-prediction by WALE corresponds to an under-prediction by StSp and StTe, and vice versa. However, the mismatch at velocity maximum clearly indicates that StSp and StTe are better models for capturing the velocity fluctuation statistics than WALE or the other models. The vorticity fluctuation profiles display more deviation between models and reference. A clear under-prediction for ω_y is seen for all models while for ω_x the maxima is well captured by StSp and StTe while the minima is better capture by the WALE model. A better profile is obtained for StSp and StTe as we approach the centre of the channel. For ω_z near wall fit is accurate for all the models while an over-prediction is seen as we move towards the centre of the channel for all models except WALE.

3.2 Flow around a Circular Cylinder at Re $\sim$ 3900

Flow around a circular cylinder in the regime of transitional flow displays numerous turbulent characteristics which need to be captured by a simulation in order to be accurate. This combined with the availability of validated experimental and numerical data sets makes cylinder wake flow at Re $\sim$ 3900 an interesting case study for LES models. The work of Parnaudeau [21] provides a PIV (PIV - Parn) and high resolution LES (LES - Parn) reference data set at this Re. Once again a coarser representation of the grid (16 times cheaper than the LES reference) is employed for the model study to keep in line with the cost effective viewpoint for LES. The simulation parameters for the LES and the references are given in table 3

Incompact3d is used to perform the simulation with the inclusion of an Immersed Boundary Method (IBM) in order to account for the presence of the solid cylinder in the flow via a forcing. For more details on the application of IBM within incompact3d please refer to [21, 3]. The cylinder is placed 5D from the streamwise (x) inlet and in the centre of the lateral (y) domain. The constant for Smag and StSm are fixed at 0.1 [20] and a spatial neighbourhood of $7 \times 7 \times 7$ is used for StSp model. For the case of wake flow around a cylinder at the resolution under study, the WALE model was found to be unstable and hence no results are shown for the same. StTe model also was observed to perform poorly for this flow - this could be attributed to the slow variation of the flow field in time especially in the wake of the cylinder. A long temporal neighbourhood might be necessary to accurately model the correlation tensor for StTe but this is not feasible computationally due to high memory requirements. Hence, StTe statistics have also been omitted from the model study.

The statistics are obtained, after an initial convergence period, for 28000 time steps, corresponding to $\sim$ 16 vortex shedding cycles, and are averaged along the spanwise (z) direction. While many statistical

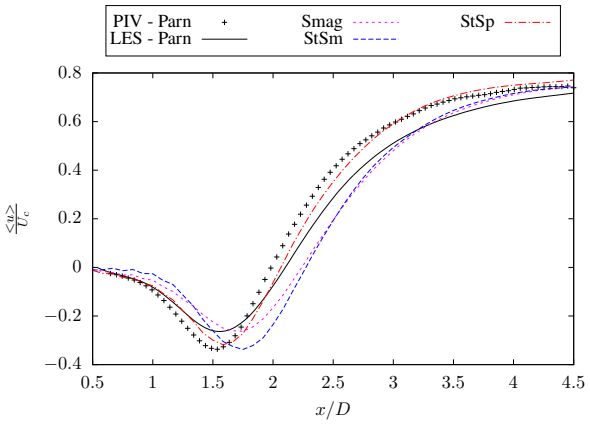

FIGURE 4 – u profile along the streamwise centerline.

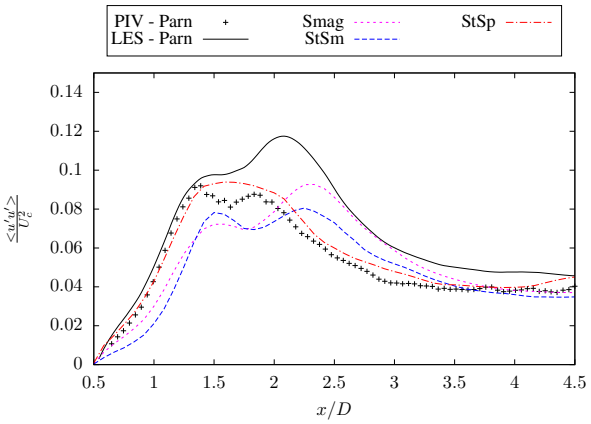

FIGURE 5 – u' profile along the streamwise centerline.

Model	PIV - Parn	LES - Parn	Smag	StSm	StSp
L_r/D	1.51	1.56	1.75	1.75	1.58

TABLE 4 – Wake recirculation length behind the cylinder.

comparisons can be realised (such as mean velocity profiles, fluctuating velocity profiles, and velocity fluctuation cross component profiles all along the lateral direction) the mean (u) and fluctuating (u') streamwise velocity profile along the streamwise centreline displays maximum deviation between the models and hence have been analysed. The u profile along the centreline is shown in figure 4 while the u' profile is shown in figure 5.

An important yet volatile parameter in cylinder wake flow is the size of the recirculation region behind the cylinder - this is the region of the flow behind the cylinder with a strong reversing flow where the vortices start to form. The length of this zone is characterised by the minima in the u profile along the centerline. The recirculation length for each model is tabulated in table 4. Smag and StSm recirculation length display 16% error as compared to the 4.6% seen for StSp. In addition, StSm and StSp better capture the PIV minima as compared to Smag.

In the u' profile, none of the models including the LES reference accurately match the two peak with a stronger initial peak profile of the PIV reference. StSm displays equal peaks but offset by a large value while Smag captured neither the position nor the magnitude accurately. StSp model captures the magnitude well but fails to capture the dual peak nature of the statistics. StSp matches well with the PIV statistics even beyond the recirculation region. It is important to mention here that the statistics for the lateral velocity profiles also display similar comparison with StSp matching better than Smag or StSm.

The statistical comparisons have shown that the models under location uncertainty perform well for both channel flow and wake flow. StSm, based on the same formulation as Smag, also performs marginally better than Smag. This improvement could be the result of the velocity bias which is the major difference between the two models. It is, thus, of interest to quantify, via isocontours, the region where this bias is in effect and the magnitude of this bias. Figure 6 shows the isocontours for SGS dissipation (shown in yellow) and the velocity bias contribution (shown in red). The region of effect for the velocity bias is clearly seen in the shear layers and within the recirculation zone - this is the region where a statistical

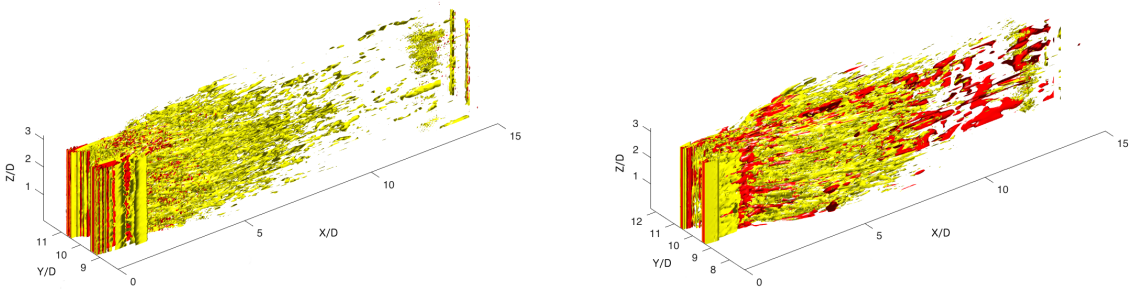

(a) StSm, (b) StSp,

FIGURE 6 – Iso-contours of SGS terms for the streamwise direction (x) with yellow iso-surface for dissipation at 0.002 and red for velocity bias at 0.001

difference is observed between the models under location uncertainty and Smag. This is indicative of the corrective nature that the velocity bias plays and its importance when performing an LES - MacInnes and Bracco [14] conclude similarly in their work where they analysed the effect of this velocity drift and stated its importance in stochastic models for accurate results. In StSp isocontours, the spatial extent for the velocity bias is much larger in comparison with StSm. The contribution extends downstream of the cylinder while in StSm this is limited to within 3D from the cylinder.

4 Conclusion

The models under location uncertainty developed by Memin [16] have been shown to yield improved results compared to the state of the art for two well established flows, namely channel flow at $\mathrm{Re}_\tau \sim 395$ and flow around a circular cylinder at $\mathrm{Re} \sim 3900$. The simulations have been performed on a coarser resolution under which classical LES models tend to be inaccurate. A statistical comparison with established reference data sets shows that the models under location uncertainty, with a special reference to the local variance based models (StSp and StTe), perform better than classical deterministic models such as classic Smagorinsky and WALE model. The performance of these models can be attributed to the additional velocity bias term in the stochastic form of the conservation equations, and to the stochastic form of the dissipation term. The region of effect of this velocity bias has also been quantified for wake flow - the region of effect is also the region of statistical mismatch for Smag which is better estimated by the models under locations uncertainty.

Références

[1] Bensoussan, A. and Temam, R. Equations stochastiques du type Navier-Stokes. *Journal of Functional Analysis*, 13(2) :195–222, 1973.

[2] Deardorff, J. W. The use of subgrid transport equations in a three-dimensional model of atmospheric turbulence. *J. Fluids Eng*, 95(429-438) :181, 1973.

[3] Gautier, R., Laizet, S., and Lamballais, E. A DNS study of jet control with microjets using an immersed boundary method. *International Journal of Computational Fluid Dynamics*, 28(6-10) :393–410, July 2014.

[4] Gent, P.R. and Mcwilliam, J.C. Isopycnal mixing in ocean circulation models. *Journal of Physical Oceanography*, 20(1) :150–155, 1990.

[5] Germano, M., Piomelli, U., Moin, P., and Cabot, W.H. A dynamic subgrid-scale eddy viscosity model. *Physics of Fluids A : Fluid Dynamics*, 3(7) :1760, 1991.

[6] Gronskis, A., Heitz, D., and Mémin, E. Inflow and initial conditions for direct numerical simulation based on adjoint data assimilation. *Journal of Computational Physics*, 242 :480–497, June 2013.

[7] Harouna, S. K. and Mémin, E. Stochastic representation of the Reynolds transport theorem : revisiting large-scale modeling. *arXiv preprint arXiv :1611.03413*, 2016.

[8] Holm, D. D. Variational principles for stochastic fluid dynamics. *Proceedings of the Royal Society A : Mathematical, Physical and Engineering Sciences*, 471(2176) :20140963–20140963, March 2015.

[9] Kraichnan, R.H. The structure of isotropic turbulence at very high Reynolds numbers. *Journal of Fluid Mechanics*, 5(04) :497–543, 1959.

[10] Laizet, S. and Lamballais, E. High-order compact schemes for incompressible flows : A simple and efficient method with quasi-spectral accuracy. *Journal of Computational Physics*, 228(16) :5989–6015, September 2009.

[11] Lamballais, E., Fortuné, V., and Laizet, S. Straightforward high-order numerical dissipation via the viscous term for direct and large eddy simulation. *Journal of Computational Physics*, 230(9) :3270–3275, May 2011.

[12] Laval, J.-P., Dubrulle, B., and McWilliams, J. C. Langevin models of turbulence : Renormalization group, distant interaction algorithms or rapid distortion theory ? *Physics of Fluids*, 15(5) :1327–1339, May 2003.

[13] Lele, S.K. Compact finite difference schemes with spectral-like resolution. *Journal of computational physics*, 103(1) :16–42, 1992.

[14] MacInnes, J. M. and Bracco, F. V. Stochastic particle dispersion modeling and the tracer-particle limit. *Physics of Fluids A : Fluid Dynamics*, 4(12) :2809, 1992.

[15] Mason, P. J. and Thomson, D. J. Stochastic backscatter in large-eddy simulations of boundary layers. *Journal of Fluid Mechanics*, 242(-1) :51, September 1992.

[16] Mémin, E. Fluid flow dynamics under location uncertainty. *Geophysical & Astrophysical Fluid Dynamics*, 108(2) :119–146, March 2014.

[17] Moin, P. and Kim, J. Numerical investigation of turbulent channel flow. *Journal of Fluid Mechanics*, 118 :341, May 1982.

[18] Moser, R. D., Kim, J., and Mansour, N. N. Direct numerical simulation of turbulent channel flow up to re_τ = 590. *Physics of Fluids*, 11(4) :943–945, April 1999.

[19] Nicoud, F. and Ducros, F. Subgrid-scale stress modelling based on the square of the velocity gradient tensor. *Flow, turbulence and Combustion*, 62(3) :183–200, 1999.

[20] Ouvrard, H., Koobus, B., Dervieux, A., and Salvetti, M.V. Classical and variational multiscale LES of the flow around a circular cylinder on unstructured grids. *Computers & Fluids*, 39(7) :1083–1094, August 2010.

[21] Parnaudeau, P., Carlier, J., Heitz, D., and Lamballais, E. Experimental and numerical studies of the flow over a circular cylinder at Reynolds number 3900. *Physics of Fluids*, 20(8) :085101, 2008.

[22] Resseguier, V., Mémin, E., and Chapron, B. Geophysical flows under location uncertainty, Part I Random transport and general models. *Geophysical & Astrophysical Fluid Dynamics*, accepted for publication, 2016.

[23] Resseguier, V., Mémin, E., and Chapron, B. Geophysical flows under location uncertainty, Part II : Quasigeostrophic models and efficient ensemble spreading. *Geophysical & Astrophysical Fluid Dynamics*, accepted for publication, 2017.

[24] Resseguier, V., Mémin, E., and Chapron, B. Geophysical flows under location uncertainty, Part III : SQG and frontal dynamics under strong turbulence. *Geophysical & Astrophysical Fluid Dynamics*, accepted for publication, 2017.

[25] Robinson, C. *Image assimilation techniques for Large Eddy Scale models : Application to 3D reconstruction*. (doctoral thesis, Université de Rennes 1, Rennes, 2015.

[26] Schumann, U. Subgrid scale model for finite difference simulations of turbulent flows in plane channels and annuli. *Journal of computational physics*, 18(4) :376–404, 1975.

[27] Shutts, G. A kinetic energy backscatter algorithm for use in ensemble prediction systems. *Quarterly Journal of the Royal Meteorological Society*, 131(612) :3079–3102, October 2005.

[28] Smagorinsky, J. General circulation experiments with the primitive equations. *Monthly Weather Review*, 91(3) :99–164, 1963.